



HAL
open science

Temporal and spatial variations in crustal accretion along the Mid-Atlantic Ridge (29°-31°30'N) over the last 10 m.y.: Implications from a three-dimensional gravity study

Janet Pariso, Jean-Christophe Sempéré, Céline Rommevaux

► To cite this version:

Janet Pariso, Jean-Christophe Sempéré, Céline Rommevaux. Temporal and spatial variations in crustal accretion along the Mid-Atlantic Ridge (29°-31°30'N) over the last 10 m.y.: Implications from a three-dimensional gravity study. *Journal of Geophysical Research*, 1995, 100 (B9), pp.17781 - 17794. 10.1029/95jb01146 . insu-01928122

HAL Id: insu-01928122

<https://insu.hal.science/insu-01928122>

Submitted on 4 Aug 2020

HAL is a multi-disciplinary open access archive for the deposit and dissemination of scientific research documents, whether they are published or not. The documents may come from teaching and research institutions in France or abroad, or from public or private research centers.

L'archive ouverte pluridisciplinaire **HAL**, est destinée au dépôt et à la diffusion de documents scientifiques de niveau recherche, publiés ou non, émanant des établissements d'enseignement et de recherche français ou étrangers, des laboratoires publics ou privés.

Temporal and spatial variations in crustal accretion along the Mid-Atlantic Ridge (29°–31°30' N) over the last 10 m.y.: Implications from a three-dimensional gravity study

Janet E. Pariso and Jean-Christophe Sempéré

School of Oceanography, University of Washington, Seattle

Céline Rommevaux

Institut de Physique du Globe de Paris, CNRS, Paris, France

Abstract. We have conducted a three-dimensional gravity study of the Mid-Atlantic Ridge near the Atlantis Transform to study the evolution of accretionary processes at this slow-spreading center over the last 10 m.y. We have removed from the free-air gravity anomaly the gravity contribution of the density contrast at the seafloor and the gravity contribution of the lateral density variations associated with the cooling of the lithosphere. The resulting residual gravity anomaly exhibits substantial variation along and across the ridge axis. The residual gravity anomaly can be accounted for by variations in crustal thickness of up to 3 km. For the first two segments south of the Atlantis Transform, the midportions of the segments have been associated with thick crust and the segment discontinuities have been associated with thin crust for the last 10 m.y., suggesting the segment discontinuities act as long-term boundaries in the delivery of melt to the individual segments. In contrast, our calculations indicate that for the segments north of the fracture zone, thick crust is associated with the midportions of segments and thin crust is associated with segment discontinuities only in crust less than ~3 m.y. This result suggests that focused mantle upwelling has only recently developed north of the fracture zone. The onset of focused mantle upwelling at approximately 2–3 m.y. may be related to a change in the spreading direction which occurred between magnetic anomalies 5 and 3 (Figure 1) and resulted in changes in the geometry of the plate boundary north of the fracture zone. Cross sections of crustal thickness extracted along the midpoint traces of paleosegments show that, for a few segments, up to 2 km of gradual crustal thinning is observed. We suggest that the "apparent" crustal thinning is a result of lateral changes in mantle density associated with buoyant upwelling not predicted by the passive flow model used in our study. Variations in computed crustal thickness are observed across axis in all of the paleosegments in our study area, but are not correlated between individual segments. If these computed crustal thickness variations are due to temporal variations in melt production, this implies that there is little interdependence in the amount of melt supplied to adjacent segments.

Introduction

Geophysical and geochemical studies in recent years have clearly demonstrated that in addition to transform offsets, the mid-ocean ridge system is segmented at a scale of 20 to 100 km by nontransform discontinuities [Macdonald *et al.*, 1988]. At slow-spreading centers, such as the Mid-Atlantic Ridge (MAR), nontransform discontinuities have offsets ranging from 0 to ~40 km [Rona *et al.*, 1976; Phillips and Fleming, 1977; Searle *et al.*, 1977; Ramberg *et al.*, 1977; Rona and Gray, 1980; Sempéré *et al.*, 1990; Needham *et al.*, 1991; Gente *et al.*, 1991; Sempéré *et al.*, 1993]. Nontransform offsets delimit the fundamental accretionary units along spreading centers and thus despite their small dimensions, constitute important structural and magmatic boundaries within oceanic lithosphere.

Segments of the slow-spreading Mid-Atlantic Ridge are often characterized by quasi circular mantle Bouguer anomaly (MBA) lows [Kuo and Forsyth, 1988; Lin *et al.*, 1990; Blackman and Forsyth, 1991; Rommevaux *et al.*, 1994; Detrick *et al.*, 1995]. When the gravity effects of the cooling lithosphere are removed from the MBA, the residual gravity anomalies (RGA) form bands extending on either side of spreading segments. The presence of low-residual anomalies indicates that the midportions of the segments are underlain by low-density material, and that the discontinuities bounding the segments are underlain by comparatively denser material. Such density variations can be interpreted as resulting from crustal thickness variations (thick crust at segment midpoints and thin crust at segment boundaries), or the presence of low-density (hot) mantle beneath segment midpoints, or a combination of the two [Kuo and Forsyth, 1988; Lin *et al.*, 1990]. Theoretical studies of mantle flow beneath ridges indicate that the gravity signal associated with lateral density variations in the melting region beneath ridges is small [e.g., Scott, 1992; Rabinowicz *et al.*, 1993]. Thus crustal thickness

Copyright 1995 by the American Geophysical Union.

Paper number 95JB01146.
0148-0227/95/95JB-01146\$05.00

variations are a likely cause for a large fraction of the residual gravity anomalies observed along the Mid-Atlantic Ridge [Lin and Phipps Morgan, 1992]. The seismic refraction study of Tolstoy *et al.* [1993] confirmed to a first order that crustal thickness variations are responsible for most of the observed residual gravity signal over the 33° S segment of the MAR. Together, these results indicate that mantle upwelling and crustal accretion at slow-spreading centers are complex, three-dimensional processes.

The relationship between upper mantle processes and the segmentation of the plate boundary is poorly understood. The presence of off-axis traces of nontransform discontinuities on the flanks of the ridge indicates that segment boundaries may be maintained for periods of time in excess of several m.y. [Rona *et al.*, 1976; Schouten *et al.*, 1987; Sloan and Patriat, 1992; Sempéré *et al.*, 1995]. Existing geophysical data over the Mid-Atlantic Ridge suggest that mantle upwelling is focused beneath the middle of most spreading segments [Kuo and Forsyth, 1988; Lin *et al.*, 1990]. However, the timing, duration, and temporal stability of focused mantle upwelling beneath the MAR are fundamental parameters over which we have little observational control at present. The duration of buoyant upwelling events beneath the spreading center, and the relationship between upwelling at neighboring segments are important factors which may control the segmentation of the plate boundary. Since variations in crustal thickness are a consequence of focused mantle upwelling, the pattern of crustal thickness on the flanks of the Mid-Atlantic Ridge provides important constraints on the evolution of the segmentation of the plate boundary.

As a means of examining the processes which influence mantle upwelling, ridge segmentation, crustal construction, and their evolution at mid-ocean ridges, we have conducted a detailed geophysical survey over the flanks of the Mid-Atlantic Ridge near the Atlantis Transform over the last 10

m.y. Our investigation was conducted as a two-leg study in collaboration with the Institut de Physique du Globe de Paris as part of the French American Ridge Atlantic (FARA) program. The present study focuses on the Mid-Atlantic Ridge between 29° and 31° 30' N.

Data Acquisition

We present and analyze gravity and bathymetry data collected during two surveys along the Mid-Atlantic Ridge (Figure 1). Geophysical data over the spreading axis (< 2 Ma lithosphere) south of 30°40'N were collected during R/V *R. D. Conrad* leg RC2912 [Lin *et al.*, 1990; Purdy *et al.*, 1990; Sempéré *et al.*, 1990; Sempéré *et al.*, 1993]. Data on the flanks of the MAR south of 30° 40'N and on the axis and flanks of the spreading center north of 30° 40' N were collected in September-November 1992 aboard R/V *Maurice Ewing* (leg EW9210 [Sempéré *et al.*, 1994]). The RC2912 and EW9210 data include gravity and multibeam bathymetry (Sea Beam and Hydrosweep, respectively). The flanks of the spreading center south of our survey area between 28° and 29° N out to 10 Ma were surveyed in 1990 by the N/O *Jean Charcot* (leg SARA, Segmentation Ancienne de la Ride Atlantique) and these results are published elsewhere [Rommevaux *et al.*, 1994; Sloan and Patriat, 1992]. Because the SARA results were previously published we do not discuss these data in our analyses or interpretation. However, we do include the SARA results in Plate 1 for comparison with those from our survey area.

The coverage obtained during leg EW9210 consists of axis-perpendicular profiles with a spacing of 4-6 km. Continuous GPS coverage was obtained throughout the survey. Bathymetry data were collected using the Hydrosweep multibeam system [Chayes, 1992]. Gravity data during leg EW9210 were acquired with a Bell Aerospace Gravity Meter-3 and a Bodenseewerk KSS-30 marine gravity meter. Cross-over errors within leg

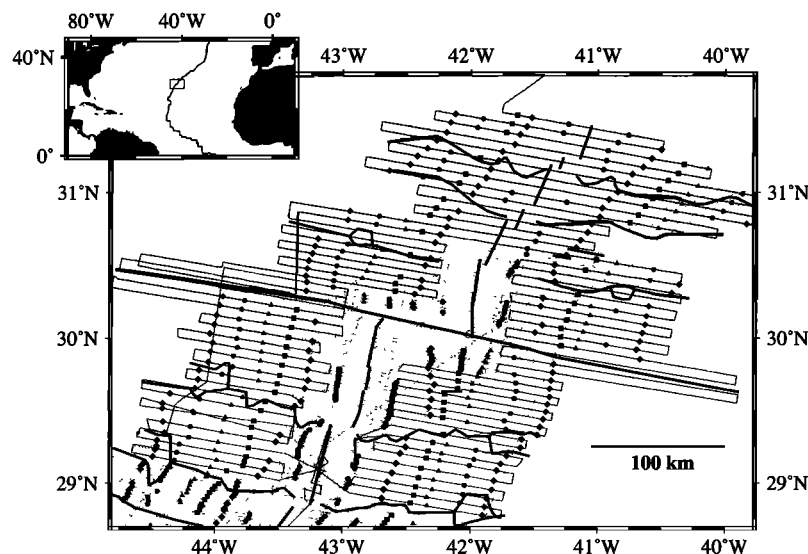


Figure 1. Location of our survey area in the North Atlantic. Ship tracks for the EW9210 data are shown by stippled black lines and ship tracks for previously published data acquired aboard the R/V *R.D. Conrad* and the N/O *Jean Charcot* are shown by the dotted shaded lines. The position of the ridge and the Atlantis Fracture Zone are shown by the heavy black lines. Magnetic anomaly picks are after Sloan and Patriat [1992] and P. Patriat *et al.*, [1995] and are shown by symbols. Solid circles are anomaly 2 (1.86 Ma), solid diamonds are anomaly 3 (3.85 Ma), solid squares are anomaly 4 (7.01 Ma), solid triangles are anomaly 4 (7.01 Ma), shaded diamonds are anomaly 5 (10.1 Ma), shaded circles are anomaly 4A (8.69 Ma).

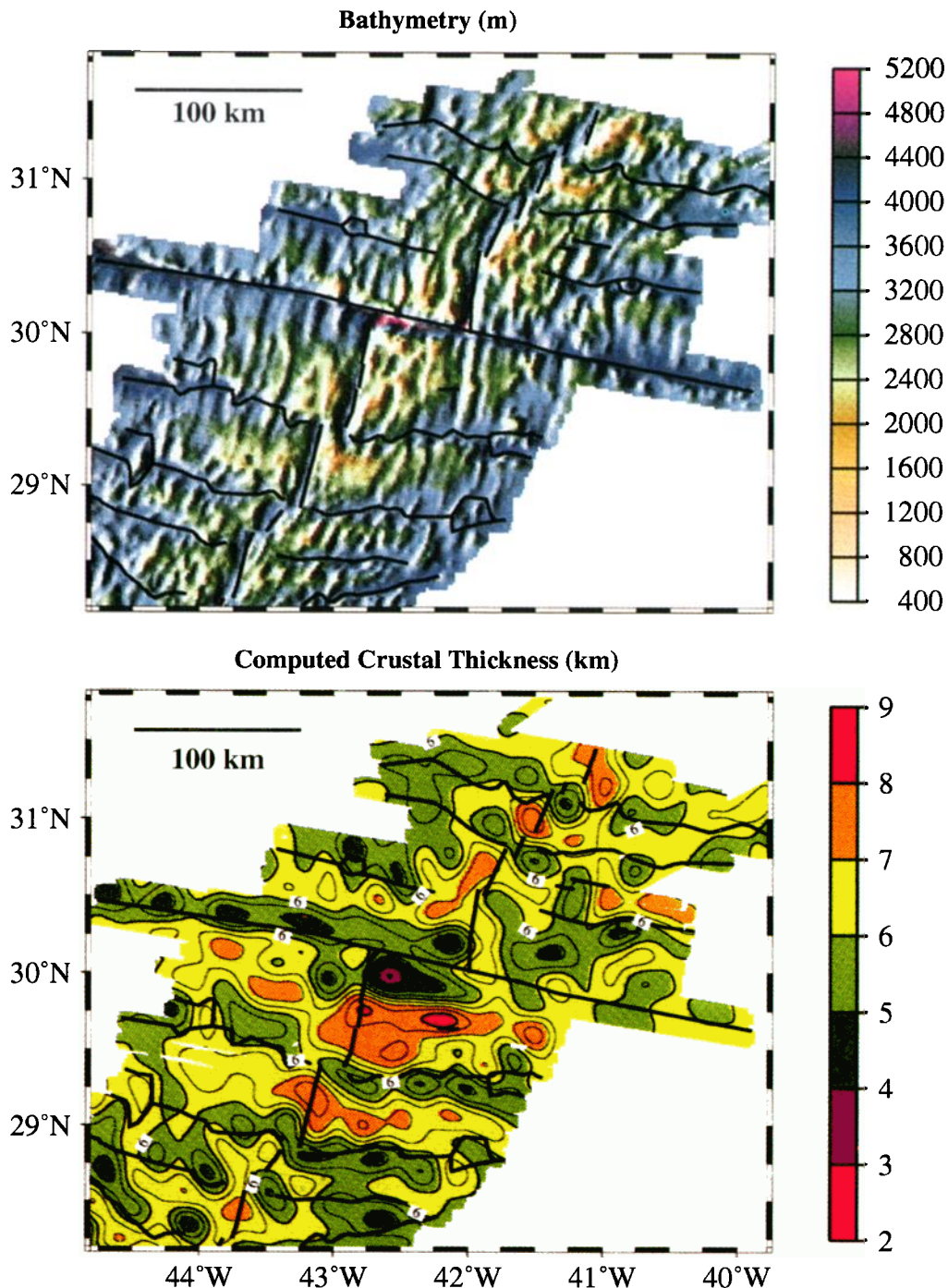


Plate 1. (top) Sea Beam [Purdy *et al.*, 1990; Sempéré *et al.*, 1990] and Hydrosweep (this study) bathymetry in our survey area. The deep valley extending from west to east at $\sim 30^\circ$ N is the Atlantis Fracture Zone. The remaining east-west troughs that extend across axis are the traces of nontransform discontinuities. (bottom) Crustal thickness computed by downward continuing of the residual gravity anomaly to a depth of 6 km below the seafloor. Values south of 29° N were not included in our discussion but were previously published by Rommevaux *et al.* [1994]. South of the Atlantis Fracture Zone, low crustal thickness values are associated with discontinuity traces out to 10 Ma. North of the Atlantis Fracture Zone, low crustal thickness values are only consistently associated with discontinuity traces for crust < 3 Ma. Contour interval is 0.5 km.

EW9210 were 1.8 ± 2.1 mGal for the KSS-30 gravimeter and 5.5 ± 8.7 mGal for the BGM-3 gravimeter. Because of the lower cross-over errors, we used the data from the KSS-30 gravimeter in our analysis. Drift during the EW9210 survey was 0.53 mGal for the KSS-30. Gravity data were collected

every 6 seconds and smoothed using a 5-point running average. The cross-over error between the RC2912 and EW9210 surveys was 1.6 ± 1.8 mGal. Thus we estimate the accuracy of our data to be better than 2 mGal. The gravity data were gridded with a minimum curvature method using splines in

tension [Smith and Wessel, 1990] at a spacing of 1.0 km and 0.78 km (north-south and east-west, respectively) to obtain a 512 by 512 grid.

Geologic Setting

The Mid-Atlantic Ridge between 29° N and 31° 30' N consists of six spreading segments separated by nontransform discontinuities and the Atlantis Transform (Plate 1 and Figure 2; [Sempéré et al., 1990; Sempéré et al., 1995]). The morphology of the ridge is characterized by a 1- to 2-km-deep rift valley. The Atlantis Transform is approximately 70 km, long and the nontransform offsets present in our survey area have lengths ranging from 5 to 20 km. Previous work identified nontransform offsets south of the Atlantis Transform near 28° 51' N and 29° 23' N [Sempéré et al., 1990]. North of the Atlantis Transform, we have identified additional nontransform offsets near 30° 33' N, 30° 50' N, and 31° 12' N. The right-stepping discontinuities and transform accommodate a 102° spreading direction along the spreading center which has a regional trend of 026°-040°. The full spreading rate within our survey area has varied from ~ 33 mm yr⁻¹ at the time of anomaly 5 to ~ 24 mm yr⁻¹ at present [Sempéré et al., 1995].

South of the Atlantis Transform, the MAR is characterized by two approximate 60-km-long segments (segments 2S and 1S in Figure 2) separated by an offset of 17 km. The on-axis bathymetric depressions associated with the discontinuities extend off-axis in the form of deep troughs that can be traced out to 10 Ma old crust. These troughs, which offset magnetic anomalies on the flank of the spreading center, are interpreted as the off-axis traces of the segment discontinuities. Both the discontinuity traces and magnetic anomaly offsets indicate that these two segments have existed for at least 10 m.y., and that they have lengthened and migrated to the south during that

time. In addition, both bathymetric data and the magnetic anomaly patterns indicate two small intra-offset ridges ceased to exist at 8 m.y. [Sempéré et al., 1995].

North of the Atlantis Transform, the morphology of the spreading center and its flanks, as well as the pattern of magnetic anomalies, indicates a complex segmentation history. North of 30° 30' N, the 040°-trending spreading center is comprised of short, en échelon ridges, 9 to 39 km in length and with offsets ranging from 8 to 15 km, located within a well-defined rift valley. On the basis of magnetic anomalies, Sempéré et al. [1995] suggested that these short ridges developed to accommodate changes in spreading direction which have taken place over the last 10 m.y. Although we have identified a total of six en échelon ridges, we have proposed that the two shortest ridges (14 and 9 km in length), located between 30° 47' N and 30° 54' N and between 31° 08' N and 31° 13' N, are intra-offset volcanic constructions which accommodate large axial discontinuities [Sempéré et al., 1994]. These two short ridges are associated with off-axis bathymetric depressions that can be traced out to about 4 Ma (50 km off-axis). We interpret these depressions as the traces of discontinuities which have separated the three existing segments (2N, 3N, and 4N) north of 30° 30' N over the past 4 m.y. As we shall describe below, our gravity results are consistent with this interpretation. The presence of deep bathymetric troughs in lithosphere older than 4 Ma., and the pattern of magnetic anomalies indicates that between 4 and 10 Ma, the MAR consisted of four segments within our survey area. However, the length and boundaries of these paleosegments differ from the present spreading center configuration.

Gravity Analysis and Results

Mantle Bouguer Anomaly

The free-air gravity anomaly is dominated by the gravitational attraction of the density contrast at the seafloor (Figure 3a). We removed from the free-air anomaly the contribution of the crust/water and crust/mantle interfaces, assuming a constant crustal thickness. We calculated the mantle Bouguer correction following the method of Prince and Forsyth [1988] and Kuo and Forsyth [1988]. We assumed a crustal thickness of 6 km, and used values of 1030, 2730, and 3330 kg m⁻³ for the density of seawater, crust, and mantle, respectively. The mantle Bouguer correction was subtracted from the free-air anomaly point-by-point along the EW9210 and RC2912 tracks at locations where we have gravity measurements. Figure 3b shows a gridded version of the MBA determined by our point-by-point subtraction.

The variations in the MBA (Figure 3b) are due to (1) crustal or mantle density variations not accounted for in our model, or (2) crustal thickness variations. Although it is possible to use a layered crustal density structure, Prince and Forsyth [1988] have shown that in a similar tectonic environment, a two-layer crust, with densities of 2200 and 2900 kg m⁻³ for upper crust and layer three, respectively, results in a difference of less than 1 mGal in the mantle Bouguer correction. Although the youngest lithosphere is covered with little or no sediment, sediment ponds are likely to be present in the bathymetric depressions on the flanks of the ridge (Figure 2). Since we do not have a measure of the true depth to basement, we cannot correct for the low-density

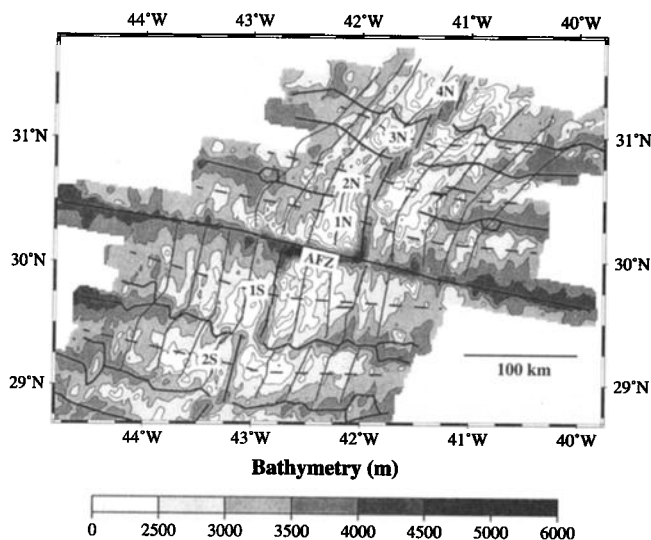


Figure 2. Bathymetric map of our survey area. Major tectonic boundaries include individual segments (medium lines, labeled 2S, 1S, 1N, 2N, 3N, 4N), the Atlantis Fracture Zone, nontransform discontinuity traces (heavy east-west lines), and paleosegment midpoint traces (heavy dashed lines). Light black lines parallel to ridge axis represent isochrons (2, 4, 6, and 8 Ma, respectively) interpreted from the magnetic anomaly pattern. Contour interval is 500 m.

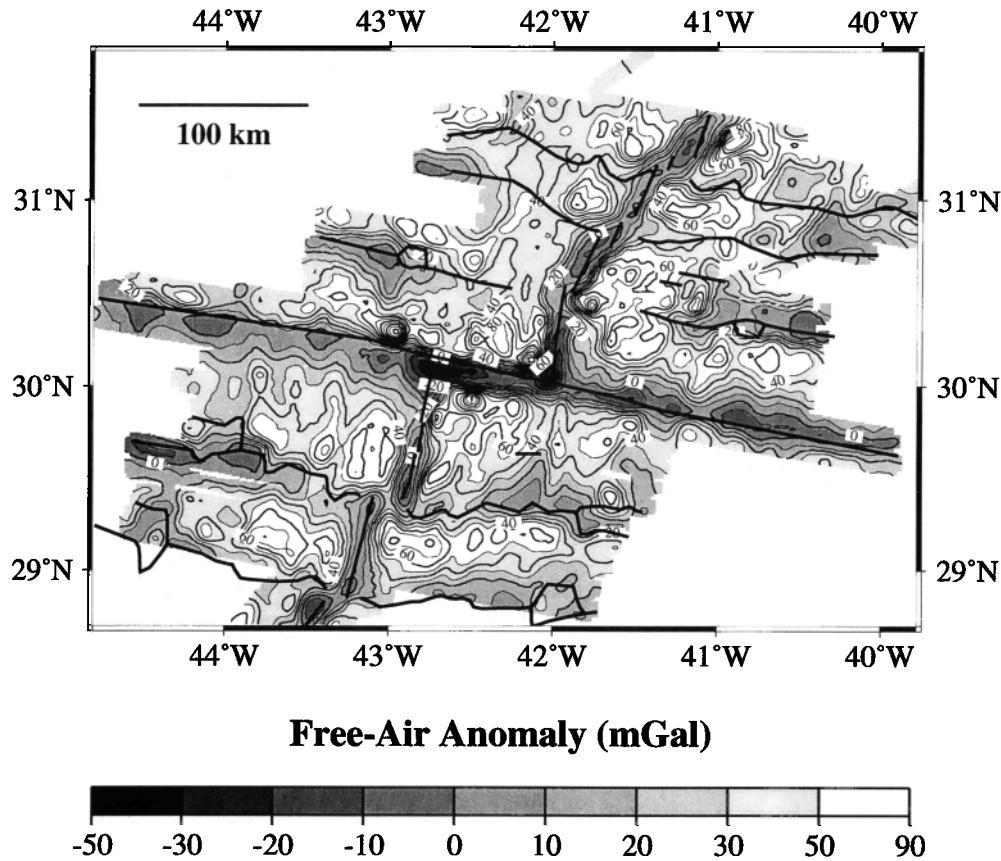


Figure 3a. The free-air gravity anomaly is dominated by short wavelength variations which reflect the density contrast at the seafloor. Contour interval is 10 mGal.

sediments which are observed primarily in the traces of discontinuities on the flanks of the spreading center. The study of *Rommevaux et al.* [1994] in the SARA area (immediately south of our study area between 28°-29°N) indicated that the largest value of sediment thickness within the older portion of the discontinuity traces is about 400 m. However, most sediment ponds in the *Rommevaux et al.* [1994] study have thicknesses of 100-200 m and their contribution to the free-air anomaly is less than, or of the order of, the uncertainty in our data. The error in the calculation of the mantle Bouguer correction obtained by not taking into account the thickest sediment ponds is of the order of 3-5 mGal [*Rommevaux et al.*, 1994]. Because we do not account for sediments, which have a lower density than the crust in our calculations, we over estimate the Bouguer correction and under estimate the MBA values over the oldest basins (> 8 Ma) within our survey area.

The MBA is characterized by a series of closed-contour ("bull's eye") lows, which are generally centered over the midportions of the individual spreading segments, and a long wavelength increase in the anomaly with age, which is due to the density increase associated with the cooling of the lithosphere with age (Figure 3b). The MBA lows form a near-linear trend of 36° from north to south in our survey area. Our off-axis coverage of the first two segments south of the Atlantis Transform shows that the low MBA values associated with the midportion of the segment and the higher MBA values associated with the discontinuities extend off-axis. We note that the trace of the MBA high is slightly offset from the trace of the bathymetric low that defines the discontinuity traces.

The pattern of low MBA values at the mid-portion of segments and high MBA values associated with segment discontinuities is also present over the four segments north of the transform, but it extends about 20 km off-axis (~2 Ma old crust). This pattern of MBA variations is not observed over the two short, volcanic ridges located along axis between segments 2N, 3N, and 4N, justifying our interpretation that they are intra-offset volcanic ridges.

Residual Gravity Anomaly

We followed the method of *Kuo and Forsyth* [1988] to remove the effect of a cooling lithosphere from the MBA to obtain the residual gravity anomaly (RGA). We calculated the gravity field due to lateral density variations in the cooling lithosphere using the passive flow model of *Phipps Morgan and Forsyth* [1988]. This model yields the temperature and flow field in a constant-viscosity mantle due solely to plate spreading (assumed to be at a constant rate). This model does not include flow produced by buoyancy effects in the mantle. We used a half-spreading rate of 12.5 mm yr⁻¹ and a thermal diffusivity (κ) of 10⁻⁶ m² s⁻¹. To predict density variations in the lithosphere from the temperature field, we computed a coefficient of thermal expansion ($\alpha = 3.55 \times 10^{-5}$ °K⁻¹) based on the average rate of subsidence in our area between 3 and 10 Ma (subsidence coefficient = 455 m Ma^{-1/2}). The density variations determined using this α value were then used to predict the variation in the gravity field at sea surface associated with our lithospheric cooling model (Figure 3c). To

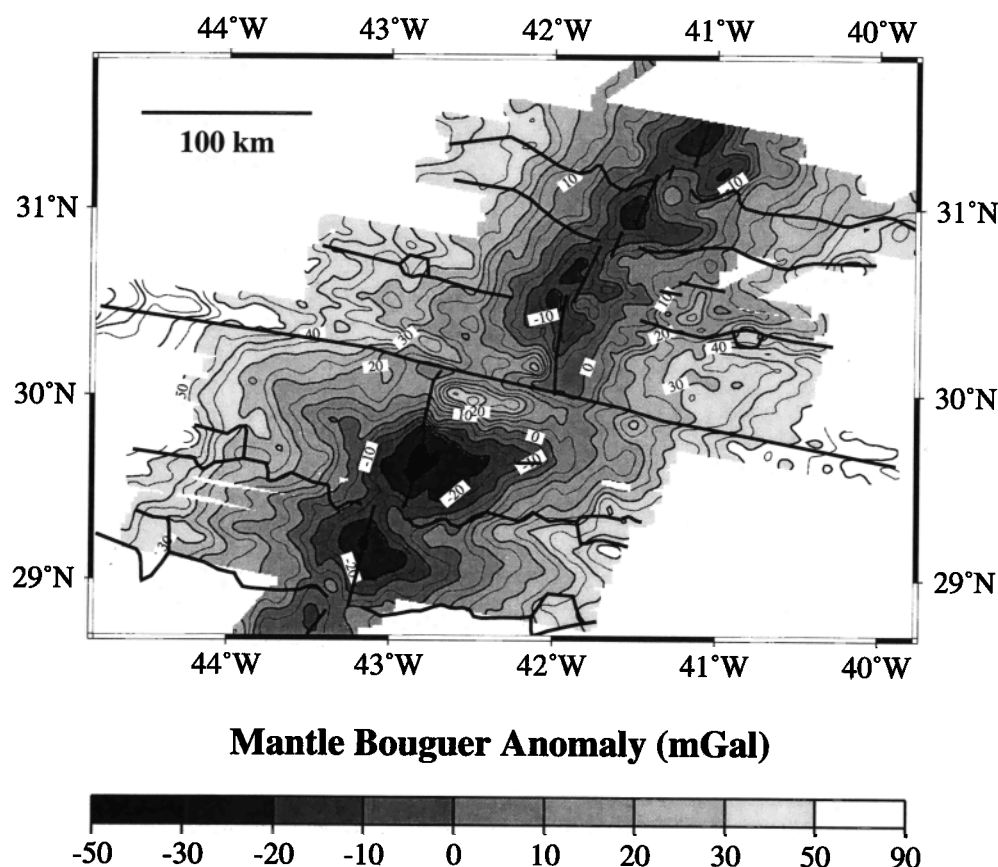


Figure 3b. The mantle Bouguer anomaly is dominated by a long wavelength increase in gravity which reflects the increase in density of the lithosphere away from the axis due to cooling. The closed-contour gravity lows over individual segments indicate regions of relatively low-density. Contour interval is 5 mGal.

obtain the RGA, we performed a point-by-point subtraction of the thermal correction from the mantle Bouguer anomaly at trackline locations where we have gravity measurements. Figure 3d shows a gridded version of the point-by-point subtraction.

Similar to the MBA, the RGA shows that well-developed lows are present over the midportions of the two segments immediately south of the Atlantis Transform. The gravity lows extend off-axis to the edge of our survey area. High RGA values are observed associated with, but slightly offset from, the segment discontinuities south of the Atlantis Transform and can be traced well to the edge of our coverage. There is no anomalous gravity signature associated with the two intra-offset ridges identified in crust 8 - 10 Ma. The RGA north of the Atlantis Transform also exhibits low values centered near (but not always directly beneath) the midportions of segments 1N-2N, 3N and 4N. However, in contrast to the segments south of the Atlantis Transform, the residual gravity anomaly lows extend only ~ 20 km off-axis.

Computed Crustal Thickness

To investigate possible crustal thickness variations within our survey area, we assumed that the gravity residual, remaining after the effects of the density contrast at the seafloor and lithospheric cooling were removed from the free-air anomaly, was due only to variation in topography at the Moho. Moho topography was calculated by downward

continuation of the RGA to a depth of 6 km below the seafloor on a 512 by 512 grid. Because downward continuation is unstable at short wavelengths, we applied a low-pass filter with a cutoff wavelength of 25 km and a cosine taper to 35 km. We calculated crustal thickness using values of Moho topography and bathymetry at trackline positions where we have gravity measurements. Plate 1 shows a gridded version of the crustal thickness values (filtered to remove the short wavelengths introduced by bathymetry). The crustal thickness values show significant variations (up to 3 km) in our study area (Plate 1). The computed crustal thickness variations correspond to RGA variations of 10 - 20 mGal (both parallel and perpendicular to the ridge) and are thus well above the noise level of our measurements. Our results indicate that for the two segments south of the Atlantis Transform, the pattern of thick crust associated with the midportions of segments and thin crust associated with segment discontinuities is maintained out to a crustal age of 10 Ma. For segments north of the fracture zone, crustal thickness maxima are observed near the central portions of segments and crustal thickness minima are present near the discontinuities only to ~20 km off-axis (~2 m.y.). For crust older than 2 m.y., crustal thickness variations do not correlate well with the pattern of segmentation observed on axis.

In addition to along-axis changes in crustal thickness, significant variations are also present across axis (Plate 1, Figure 4). First, undulations in calculated crustal thickness are observed on the flanks of individual segments. At wavelengths

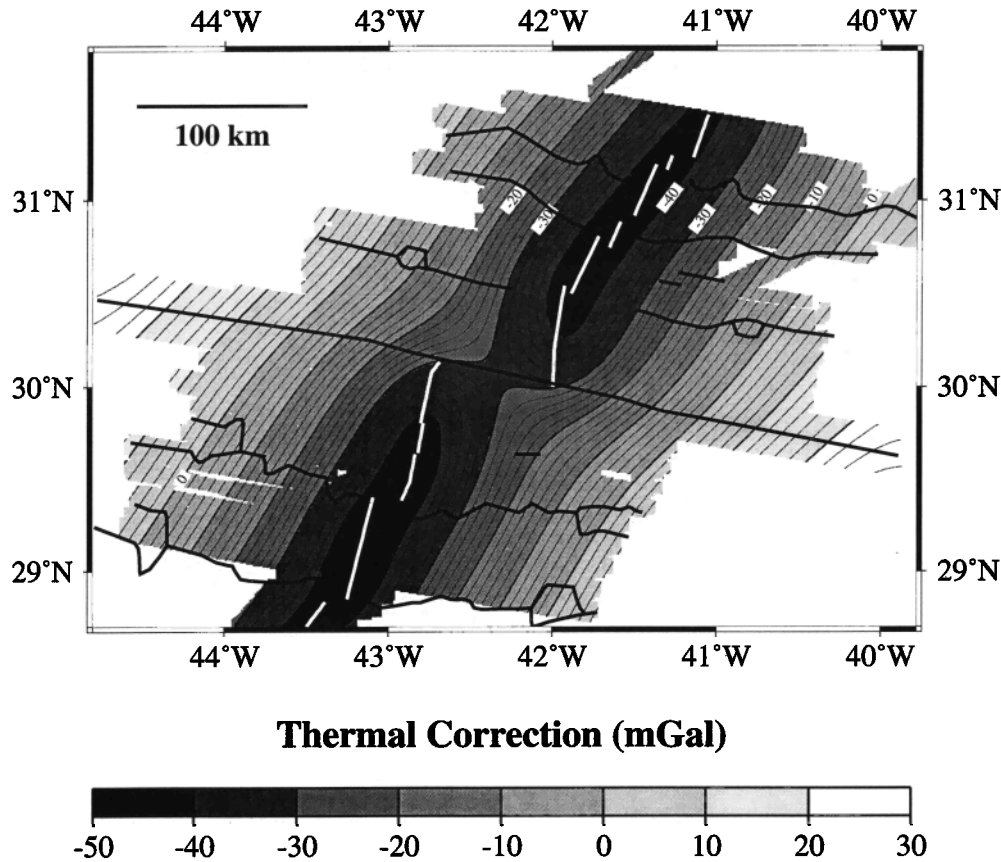


Figure 3c. The gravity signal at sea surface predicted from lithospheric cooling based on the passive flow model of *Phipps Morgan and Forsyth* [1988]. Note that although cooling associated with the transform has an important effect on the predicted gravity field, there is no discernable change in predicted gravity field associated with nontransform discontinuities. Contour interval is 2 mGal.

on the order of 40 km (~3 m.y.), these undulations have amplitudes between 1-2 km and in general are not symmetric about the ridge axis (except for segment 1S). Second, for the two segments adjacent to the Atlantis Fracture Zone (1S and 1N), the computed crustal thickness is asymmetric with respect to the axis. The midpoint trace of the west flank of segment 1N is generally 0.5 - 1.0 km thicker than that of the east flank and, the midpoint trace of the east flank of segment 1S center is generally 0.5 - 1.0 km thicker than that of the west flank. This suggests a long-term, across-axis asymmetry in crustal production, tectonism, or accretion for the two segments adjacent to the transform fault. Third, several of the segment flanks exhibit "apparent" crustal thinning, of the order of 1-2 km, with age.

Interpretation

In our calculation of crustal thickness, we have assumed that the residual gravity anomaly is due solely to topography at the Moho. Theoretical models of mantle flow beneath ridges, including various sources of buoyancy, indicate that density variations in the mantle cannot account for the observed range of variation in the RGA along the axis of the Mid-Atlantic Ridge [Lin and Phipps Morgan, 1992; Scott, 1992; Rabinowicz et al., 1993]. Thus the primary source of variability in along-axis, residual gravity appears to reside in crustal thickness variations and/or lateral density variations in the crust. However, variations in melt fraction retained and in

mantle density due to depletion may explain some of the across-axis variations in residual gravity [Scott, 1992; Su and Buck, 1993].

Three studies have indicated that crustal thickness estimated using gravity data compares well, to a first order, with crustal thickness measured using seismic refraction [Morris and Detrick, 1991; Tolstoy et al., 1993; Detrick et al., 1995]. However, discrepancies between the seismic and gravity determination of crustal thickness do appear in these studies. For example, crustal thickness calculated using gravity compares well with that determined using seismic refraction south of the Kane Fracture Zone, except in the immediate vicinity of the transform [Morris and Detrick, 1991]. This discrepancy was attributed to unusually low crustal densities in the vicinity of the fracture zone. Similarly, Tolstoy et al. [1993] showed that crustal thickness variations computed using gravity data for a segment located near 33° S on the Mid-Atlantic Ridge agree to a first order with those seismically determined. However, their study indicated that approaching segment discontinuities, crustal thinning and a decrease in crustal density are both required. This result was confirmed by Detrick et al. [1995] near the Oceanographer Transform. In the following discussion, we use the residual gravity anomaly to infer variations in crustal thickness. It is important to keep in mind that the observed variations in the residual gravity anomaly may also be due, in part, to variations in crustal or mantle densities.

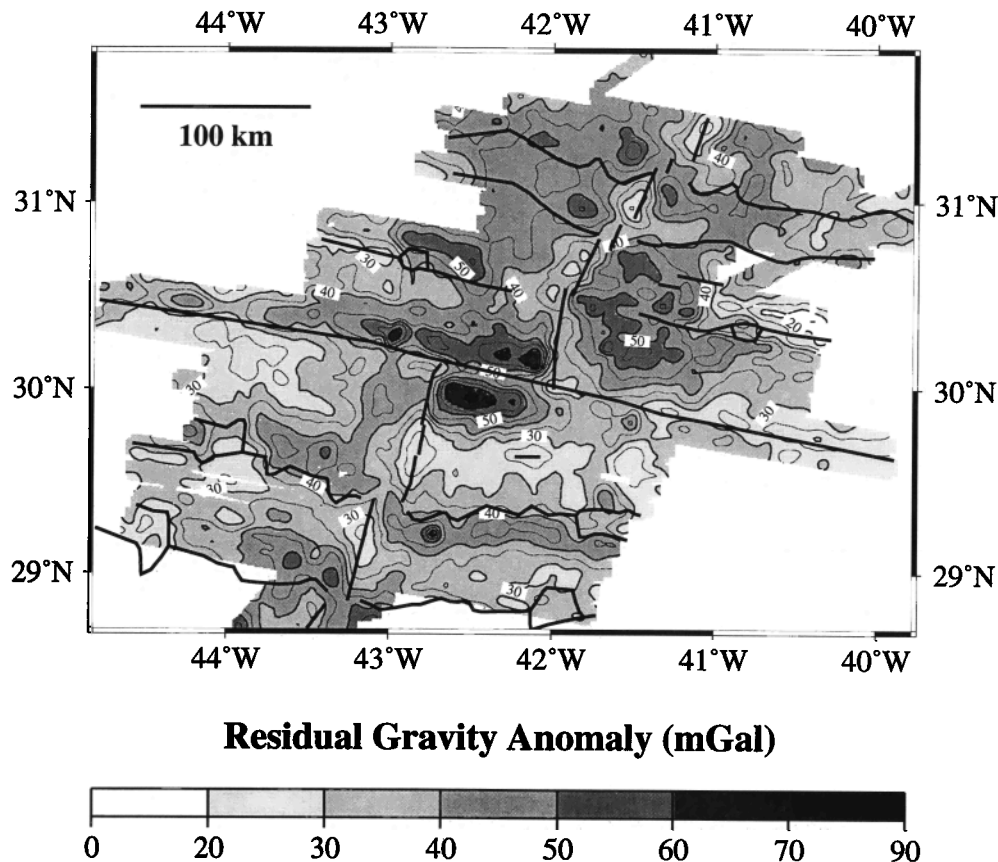


Figure 3d. The residual gravity anomaly (RGA) was calculated by subtracting the gravity field due to lithospheric cooling from the Bouguer anomaly. South of the transform, off-axis traces of segment discontinuities are associated with relatively high RGA values. North of the transform the off-axis traces of segment discontinuities are not correlated with low RGA values. Contour interval is 5 mGal.

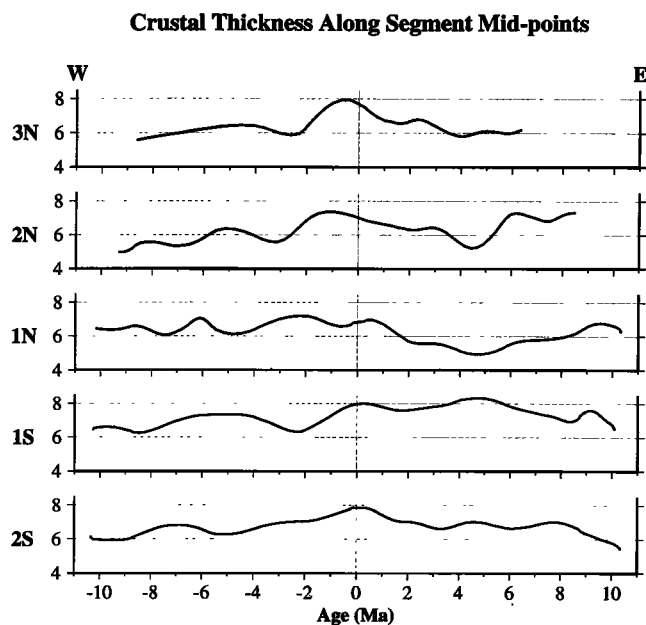


Figure 4. Cross sections of computed crustal thickness along segment mid-point traces of individual spreading segments. Profiles 2S, 2N west, and 3N suggest that gradual crustal thinning has taken place. Note that although many profiles show undulations in computed crustal thickness, these variations are poorly correlated between individual segments.

Spatial Variations in Crustal Structure

The variations in crustal thickness that we have computed based on the residual gravity anomaly reflect to first order the present and past pattern of segmentation of the plate boundary within our survey area (Plate 1). In general, the fracture zone and nontransform discontinuities are associated with thin crust (~5-6 km), while the midportions of segments are associated with thicker crust (~6-8 km). However, we note that the pattern of gravity anomalies (and thus computed crustal thickness) is complex. The thinnest crust is often slightly offset (to the north or south) from the deepest portion of both the fracture zone and the discontinuity traces. For segments 1N and 2N, the thickest crust is slightly offset to the east and west, respectively, from the ridge axis itself. For segments south of the Atlantis Transform (1S and 2S), the pattern of thick crust at the segment midpoint and thin crust beneath the segment ends is maintained out to 10 Ma.

Previous studies [Kuo and Forsyth, 1988; Lin et al., 1990] have suggested that the low-residual gravity values over the centers of individual spreading segments were expressions of focused mantle upwelling. If this interpretation is correct, our results indicate that focused mantle upwelling has been maintained for at least the last 10 m.y. within segments 1S and 2S. In the SARA area, immediately south of our survey area, previously published results show that focused upwelling has also existed at least for the last 10 m.y. (Plate 1, Rommevaux et al. [1994]). Thus segment discontinuities function as long-lived boundaries in the delivery of melt to individual spreading

segments, or they constitute the lithospheric response of long-lived focused mantle upwelling on time scales up to 10 m.y.

Crustal thickness variations along the four segments identified north of the Atlantis Transform are very complex. On axis, the midportions of these segments are associated with high values of computed crustal thickness, but the loci of thickest crust are not necessarily centered directly under the axis. Our bathymetry data indicate that the neovolcanic zones north of 30° 30' N consists of en échelon ridges located within the rift valley. Although our bathymetric data suggest that even the two shortest ridges (30° 48' N-30° 55' N and 31° 11' N-31° 13' N) are the product of constructional volcanism, these short ridges are associated with RGA highs that extend off-axis and correspond to bathymetric troughs. Thus we infer that these short ridges accommodate axial discontinuities associated with off-axis traces. These intra-offset ridges may evolve into spreading segments in the future. Bathymetry, magnetics, and gravity data suggest that segments 1N and 2N may be in the process of merging into one segment. The magnetic anomaly pattern indicates that there has been a substantial decrease in the length of the offset at the 1N/2N discontinuity over the last 10 m.y. (Figure 1, *Sempéré et al.* [1995]). Although the discontinuity trace is associated with a bathymetric depression in 4-10 Ma crust (> 50 km off-axis), only a minor topographic disruption is observed at the 1N/2N boundary in crust < 4 m.y. (< 50 km from the axis). Further, crust formed at the 1N/2N discontinuity is only associated with minor thinning for ages < 3 Ma. These observations suggest that in the last 3-4 m.y., the discontinuity between segments 1N and 2N has not been a significant boundary in the geometry of mantle upwelling.

North of the fracture zone, the pattern of thin crust associated with segment discontinuities and thick crust associated with segment midpoint holds reasonably well for crust less than ~ 3 m.y. (with the exception of the 1N/2N discontinuity). Although there are substantial crustal thickness variations from ~ 3 to 8 m.y. (values range from 5 to 8 km), the maxima and minima in crustal thickness exhibit a poor correlation with the paleosegmentation pattern (Figures 1 and 3d). A change in the paleosegmentation pattern can be identified at about 3 - 4 m.y. north of 30° 30' N and may be related to a progressive, clockwise rotation of the spreading direction from ~93° to ~106° between magnetic anomalies 5 (~10.1 Ma) and 3A (~5.7 Ma) [*Sempéré et al.*, 1995]. This reorganization of the plate boundary appears to be contemporaneous with the accretion of a more complex crustal structure which does not exhibit bands of thin and thick crust at high angles to the spreading axis.

The lack of association of the MAR between 30° 30' N and 31° 30' N with an organized pattern of residual gravity anomalies, may be explained in two ways. First, the changing segmentation pattern associated with the reorganization of the plate boundary may have resulted in crustal thickness variations which are smaller in scale than we can resolve with our analysis (~ 25 km). Alternatively, the reorganization of the plate boundary may result in mantle upwelling which is not focused in a three-dimensional sense. This effect of the reorganization appears to only have affected spreading segments located away from the Atlantis and Hayes Transforms. Indeed, *Detrick et al.* [1995] have shown that the segment located between 33°N and the Hayes Transform is associated with a pattern of residual gravity anomalies akin to that south of 30° 30'N.

Although the crust is thinner near the traces of both transform and nontransform discontinuities, the loci of thinnest crust do not coincide with the deepest part of the traces. Our calculations show that on the west side of the Atlantis Fracture Zone, the thinnest crust is located beneath the north wall of the fracture zone rather than below the deepest part of the fracture zone valley (Plate 1). Similar results have been obtained in previous gravity studies over fracture zones [*Prince and Forsyth*, 1988; *Blackman and Forsyth*, 1991]. Away from the fracture zone in our study area, zones of gravity-inferred thin crust (or highest residual gravity) are observed along the traces of nontransform discontinuities. The morphology of the discontinuities is generally asymmetric in nature [*Rommevaux et al.*, 1994]. The side of the trace which is formed at the "inside corner" of the discontinuity dips steeply toward the offset trace, while crust formed at the outside corner dips more gently. The thinnest crust is found along the steep wall rather than the deepest portion of the trace. The thin crust found under the steep walls of fracture zones and discontinuities may be a result of the combined effects of a diminished magma supply, resulting from their location at the distal end of an upwelling plume, and tectonic extension. Alternatively, our computed crustal thickness values may be in error because the density of the crust and mantle beneath the deepest part of the discontinuity may be lower than that used in our model. For example, localized serpentinization could reduce the density of the mantle or crust underlying the deepest part of the discontinuity trace.

A striking feature of our result is the east-west asymmetry in crustal thickness along the trace of the Atlantis Fracture Zone. Crust east of the Atlantis Transform is, on average, 1 km thicker than crust west of it (Figure 5). Seismic refraction work has shown that crustal thickness along the Kane Fracture Zone is also variable, with 2-to 3-km-thick crust observed along the eastern portion of the fracture zone, but 6-km-thick crust along the eastern part of the transform [*Cornier et al.*, 1984]. These results suggest that transform faults are not necessarily magmatically starved during the process of crustal accretion and indicate that, while crustal thinning near and within fracture zones is common, crust of normal thickness can also be formed. In the case of the crust formed along the eastern portion of the Atlantis fracture zone, the normal crustal thickness values (approximately 5-6 km) observed may be due to an unusually robust magma supply at segment 1S. Our results indicate that the crustal thickness values computed for segment 1S are consistently higher than values from the other segments in our study area (Plate 1 and Figure 4). In addition, bathymetry data and computed crustal thickness values show that crustal production has consistently been higher on the east flank of segment 1S than on the west flank. The high production of crust on the east flank of segment 1S may have caused volcanic overprinting in the fracture zone valley, and resulted in high crustal thickness values.

In addition to asymmetry in computed crustal thickness values along the transform itself, there is a clear east-west asymmetry in thickness for crust produced at the two segments adjacent to the transform (Figure 4). Crustal thickness values on the west flank of segment 1N are generally 0.5 - 1.0 km higher than that on the east flank, and the crustal thickness values on the east flank of segment 1S center are generally 0.5 - 1.0 km thicker than that of the west flank. This result suggests long-term across-axis asymmetry in crustal production or tectonism for the two segments adjacent to the

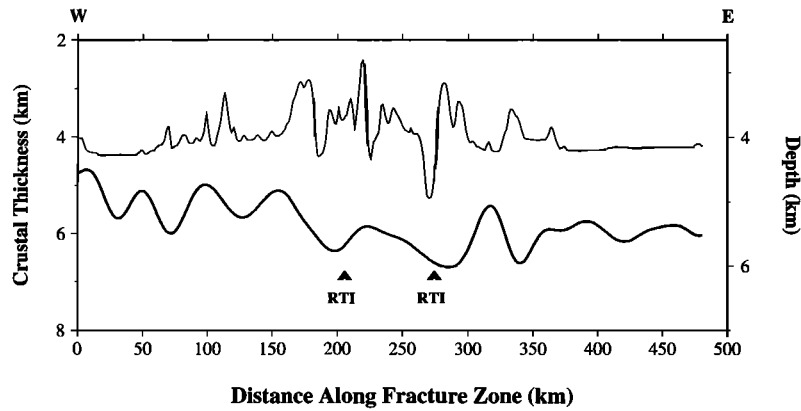


Figure 5. Cross sections of bathymetry (thin line) and computed crustal thickness (thick line) along the Atlantis Fracture Zone. Note that the crust underlying the east side of the fracture zone is generally thicker than that underlying the west side.

transform fault. Using three-dimensional numerical modeling techniques, *Rabinowicz et al.* [1993] showed that the presence of a transform fault results in the generation of a toroidal flow field which can shift upwelling plumes away from the ridge crest. Such a mechanism could account for the high crustal production on the west flank of segment 1N and the east flank of segment 1S.

Temporal Variations in Crustal Structure

To examine the temporal variation in crustal structure along axis, we have plotted cross sections of bathymetry and computed crustal thickness along isochrons on both the east and west flanks of the ridge in our study area (Figures 6a and 6b). The isochrons were determined using crustal ages interpolated from magnetic anomaly data (Figures 1 and 2, *Sempéré et al.*, 1995). These plots show that there are up to 3.5 km of variation in crustal thickness on axis. If we exclude the fracture zone, there are still 3 km of variation in crustal thickness along axis between segment midpoints and discontinuities. Examining crustal thickness cross sections along isochrons, it is clear that the most salient crustal thickness variations are consistently associated with the segment boundaries. For the southern segments (1S and 2S), the pattern of thin/thick crust associated with discontinuities/segment midpoints is very consistent out to 8 Ma. North of the Atlantis Transform, this correlation between crustal thickness and position along the segment is only observed for crust which is < 3 Ma. For example, at present, the four spreading segments north of the Atlantis Transform are associated with four centers of thick crust. However, starting at the 3 Ma isochron, the bathymetric highs which represent paleosegment midpoints, and the bathymetric lows, which define paleosegment discontinuities, are not associated with thick and thin crust, respectively. As we discussed earlier, these results suggest that between approximately 3 and 8 Ma, individual segments north of the fracture zone were not associated with focused mantle upwelling. This is likely related, or in response, to a reorganization of the plate boundary which took place between 10 and 4 Ma [*Sempéré et al.*, 1995].

We have identified the traces of the midpoints of paleosegments using a combination of the midpoint between the discontinuity traces, bathymetric highs on the flanks of

the MAR, and high values of calculated crustal thickness (Figure 2). The midpoint traces thus represent lines of maximum crustal thickness and the likely location of segment midpoints, or mantle upwelling centers, with time. Cross sections of crustal thickness along these midpoint traces

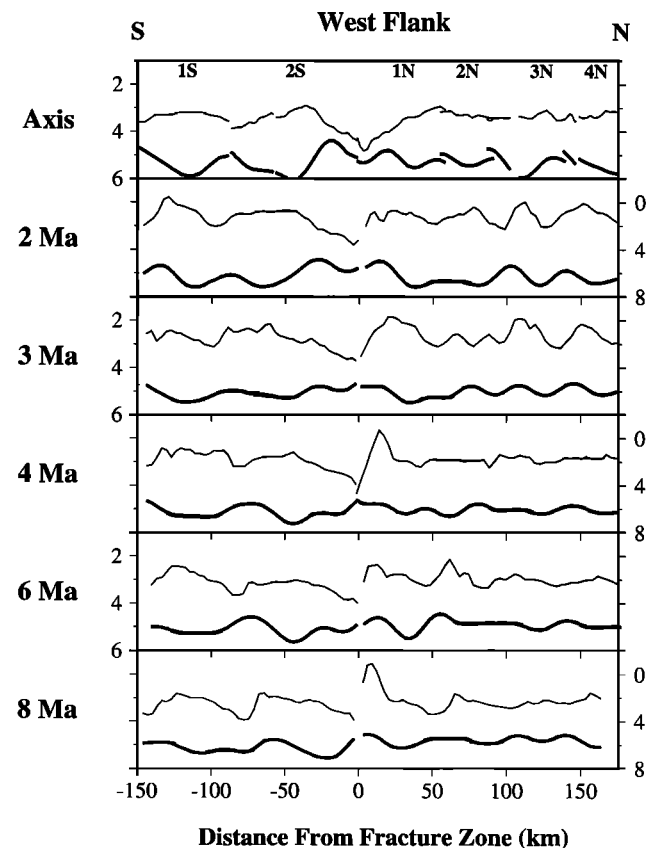


Figure 6a. Cross sections of bathymetry (thin line) and computed crustal thickness (heavy line) along isochrons on the west flank of the MAR. The bathymetry scale is on the left and the computed crustal thickness scale is on the right. For the two segments south of the fracture zone, segment discontinuities are associated with thin crust for up to 8 Ma. North of the fracture zone, segmentation boundaries are poorly correlated with thin crust in lithosphere > 3 Ma.

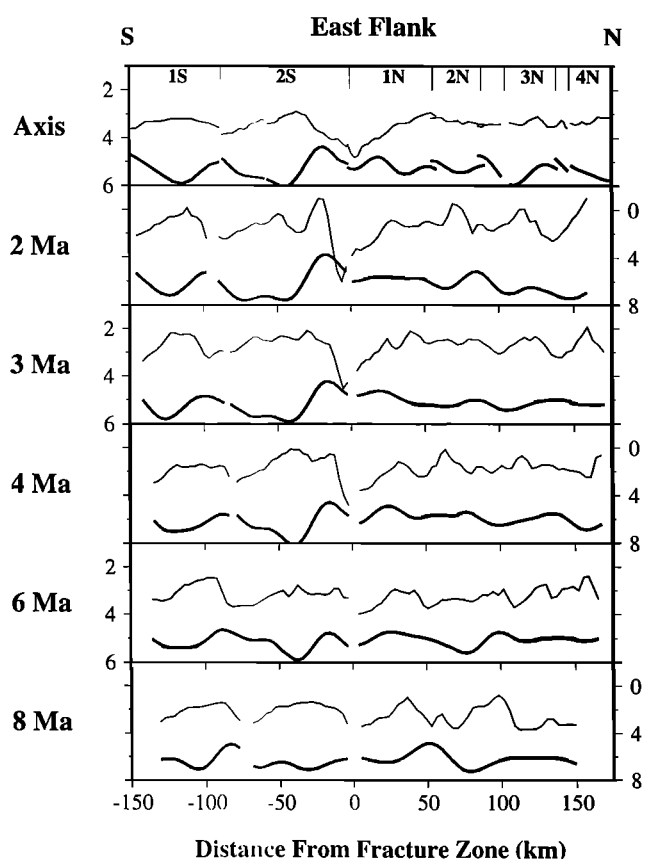


Figure 6b. Cross sections of bathymetry (thin line) and computed crustal thickness (heavy lines) along isochrons on the east flank of the MAR in our survey area. The bathymetry scale is on the left and the computed crustal thickness scale is on the right. For the two segments south of the fracture zone, segment discontinuities are associated with thin crust for up to 8 Ma. North of the fracture zone, segmentation boundaries are poorly correlated with thin crust in lithosphere > 3 Ma.

provide a measure of the temporal variation in crustal production for individual segments (Figure 4). The most notable features of the relationship between crustal thickness and time are as follows: (1) profiles 2S, 2NW, and 3N suggest gradual crustal thinning with age, (2) the cross sections of segments 2S, 2N, and 3N suggest that the crust near the axis is at least 1 km thicker than the crust off-axis, and (3) there are up to 2 km of variation in crustal thickness at a timescale of 2-3 m.y. We will address the possible causes and implications of these features in this order.

Apparent decrease in crustal thickness values with age. Profiles 2S, 2NW, and 3N extracted from grids along paleo midpoint traces exhibit gradual crustal thinning with age. The same observation can be made for a similar analysis of the gravity field over the MAR between 33° N and 40° N [Detrick *et al.*, 1995]. To investigate systematic crustal thickness variations away from the axis of the MAR, we derived the parameters of the best-fitting, linear relationship between calculated crustal thickness and distance from the axis. Since our calculated crustal thickness is largest near the axis for each profile, we also investigated the relationship between crustal thickness and distance from the axis excluding the near-axis region. When only the portions of the profiles corresponding to ages greater than 2 m.y. are considered,

apparent crustal thinning is observed on profiles 2SE, 1SE, 2NW, and 3NE. Since we did not account for the presence of sediment in our Bouguer correction, it is possible that our computed crustal thickness values are in error in older crust. However, significant sediment accumulation is only important within the bathymetric troughs of the discontinuity traces, not along the relative bathymetric highs that characterize the paleo midpoint traces. There are several other ways to explain these observations: variations in crustal production with time, active thinning of crust by tectonic extension, or a crust or mantle density structure which is slightly different than that used in our analyses. We examine in turn these possible mechanisms.

A possible source for the decrease in computed crustal thickness values observed with age over some of the spreading segments in our study area is a gradual increase with time in the magmatic budget. *Su et al.* [1994] have shown that, at slow-spreading centers, crustal production may increase with decreasing spreading rate under certain conditions. Interpretation of magnetic anomalies in our survey area show that the regional spreading rate has slowed from ~ 32 mm yr⁻¹ 10 Ma to ~ 24 mm yr⁻¹ at present. Because apparent crustal thinning is not observed ubiquitously within our area, we argue that a regional decrease in melt production with time is not the cause of our observation. However, we cannot discard local variations in melt production as the cause of our observation.

Another mechanism for gradual crustal thinning is tectonic extension and crustal denudation. For example, a simple calculation based on conservation of volume indicates that 25% extension (a moderate amount for the Mid-Atlantic Ridge; [Karson and Winters, 1992]) would result in a decrease in crustal thickness of 1.2 km from our initial reference value. Surface observations over the MAR indicate that fault throw and fault density increase toward segment offsets, suggesting that the brittle-ductile transition may be deeper near axial discontinuities [Sempéré, 1991; Shaw, 1992; Sempéré *et al.*, 1993]. In addition, teleseismic activity along the MAR is predominantly located at the distal ends of segments [Lin and Bergman, 1991]. These results indicate that if crustal thinning occurs by tectonic extension, the largest degree of thinning should occur near segment discontinuities (also see Mutter and Karson, [1992]). However, examination of our computed crustal thickness variations (Plate 1 and Figure 4) shows that the largest decrease in crustal thickness with distance from the ridge takes place along paleo midpoint traces, and that little crustal thinning occurs along the discontinuity traces. Therefore, we suggest that although extension is an important process at the MAR, the apparent long-term decrease in crustal thickness along some of the midpoint traces of segments does not have a predominantly tectonic origin.

A possible cause for the observed decrease in computed crustal thickness values with age is an error in the parameters used in our downward continuation. In this calculation, we used a constant mantle density of 3330 kg m⁻³. Since the lithosphere cools with age, it is more reasonable to use a variable crust/mantle density contrast close to the axis where lateral temperature variations are likely to be the largest. Downward continuation to Moho level using a crust/mantle density contrast which increases away from the axis according to our passive flow model results in changes in crustal thickness of the order of 100-200 m. Thus lateral density variations at the Moho associated with lithospheric cooling

can only account in part for the apparent crustal thinning with age.

The apparent crustal thinning, determined by downward continuation of the residual gravity anomaly, is ultimately due to the presence of a long wavelength increase in residual gravity away from the ridge. The passive flow model used to predict the thermal structure of the lithosphere accounts for most of the long wavelength signal observed in the mantle Bouguer anomaly. The remaining long wavelength increase in the gravity field has a relatively small amplitude (of the order of 5-10 mGal). A likely cause for long wavelength variations in gravity-inferred crustal thickness away from the axis is that our thermal model does not completely describe lateral density variations in the mantle beneath some spreading segments. The discrepancy between the passive flow model and our observations may be due to several causes.

First, the thermal structure calculated using a passive flow model depends on our choice of spreading rate, thermal diffusivity, and the coefficient of thermal expansion [Phipps Morgan and Forsyth, 1988]. Spreading rate variations, such as those observed within our study area, are not taken into account in our passive flow model. We have calculated the thermal correction using a two-dimensional lithospheric cooling model [Parsons and Sclater, 1977] and the age grid of our survey area derived from the interpretation of magnetic anomalies. Comparison between the two models shows that small variations in spreading rate do not significantly affect the thermal structure of the lithosphere. Another possibility to explain the discrepancy between the passive flow model and our observations is that the thermal diffusivity or thermal expansion coefficient values used in our calculation ($\kappa = 10^{-6} \text{ m}^2 \text{ s}^{-1}$, $\alpha = 3.55 \times 10^{-5} \text{ }^\circ\text{K}^{-1}$) may only describe part of our

study area accurately. For example, local variations in "effective" α could arise due to variable hydrothermal cooling within our study area or segment-scale variations in the latent heat released during crustal emplacement [Neumann and Forsyth, 1993]. Figure 7 demonstrates that reasonable changes in α and κ could only account for a small portion of the account for the observed discrepancy between the observed and predicted increase in gravity with age.

Because the passive flow model [Phipps Morgan and Forsyth, 1988] assumes that mantle flow is due solely to spreading plates over an isoviscous mantle, our thermal correction does not include the effects of temperature- and pressure-dependent viscosity, or thermal, compositional, and melt buoyancy. All of these factors affect the flow field, and thus the temperature structure (and ultimately the gravity field) of the mantle [Scott, 1992; Shen and Forsyth, 1992; Turcotte and Phipps Morgan, 1992; Rabinowicz et al., 1993; Su and Buck, 1993; Su et al., 1994]. Su and Buck [1993] showed that the gravity signal due to lateral variation in melt retention can be significant up to 50 km from the ridge axis (e.g., 7-8 mGal for an intermediate spreading center). Numerical models show that the magnitude of the compositional density variation in the mantle can offset the lateral density contrast due to melt retention [Scott, 1992]. Thus the gravitational effect associated with buoyant mantle flow should ideally be considered in the calculation of residual gravity anomalies. This nonpassive contribution is however difficult to predict due to our lack of knowledge of many of the physical parameters involved, such as the amount of melt retained in the mantle and mantle viscosity. This nonpassive contribution to the long wavelength variations in gravity perpendicular to the axis may be responsible for the apparent variations in crustal thickness away from the axis.

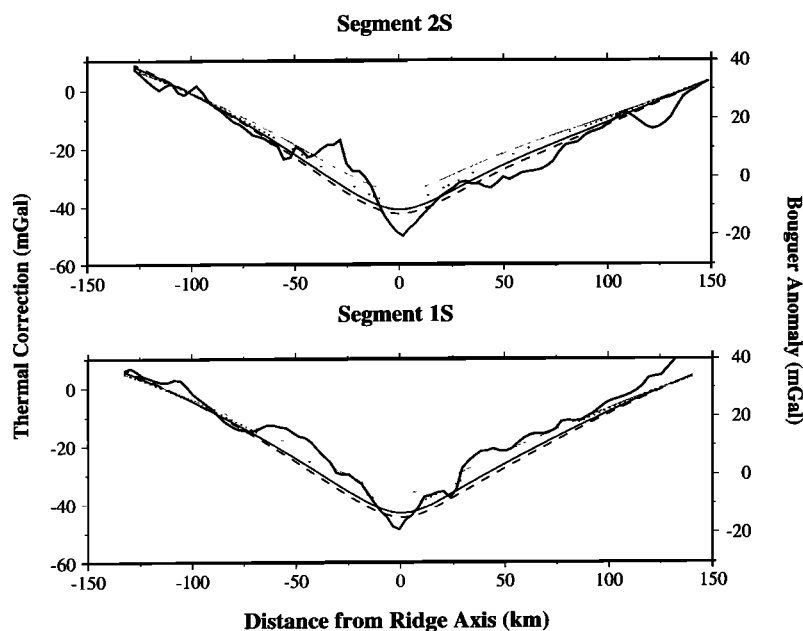


Figure 7. Thermal gravity correction compared to the Bouguer anomaly over the paleo-midpoint traces of segments 2S and 1S. The shaded line is the thermal gravity correction computed using $\kappa = 1 \times 10^{-6} \text{ m}^2 \text{ s}^{-1}$ and $\alpha = 3 \times 10^{-5} \text{ }^\circ\text{K}^{-1}$. The black line is the thermal gravity correction computed using $\kappa = 1 \times 10^{-6} \text{ m}^2 \text{ s}^{-1}$ and $\alpha = 3.55 \times 10^{-5} \text{ }^\circ\text{K}^{-1}$ (based on the local rate of subsidence, $455 \text{ m Ma}^{-1/2}$). The dotted and dashed lines were computed using $\kappa = 0.75 \times 10^{-6}$ and $1.25 \times 10^{-6} \text{ m}^2 \text{ s}^{-1}$ (respectively) and $\alpha = 3.55 \times 10^{-6} \text{ }^\circ\text{K}^{-1}$. Note that the thermal gravity corrections for segment 2S and the west flank of segment 1S match the long wavelength increase in the Bouguer anomaly reasonably well. In contrast, none of the thermal gravity corrections match the long wavelength increase in the Bouguer anomaly along the east flank of segment 1S very well.

In summary, the "apparent" crustal thinning observed with age over portions of our study area is likely to be a result of lateral changes in mantle density not predicted by the passive flow model used in our study. These lateral changes in mantle density are most likely related to buoyant upwelling and flow focusing beneath the axis, and can result in a decrease in the residual gravity field close to the spreading center. The observation that "apparent" crustal thinning is observed out to 10 Ma on some (but not all) spreading segments in our study area suggests that the nature of buoyant upwelling varies on a segment scale.

Variations in crustal thickness on a time scale of 2-3 Ma. Cross sections of crustal thickness along paleo-mid-points show significant variations in crustal thickness (up to 2 km) on a timescale of 2-3 m.y. One explanation for these variations is that they result from temporal variations in melt production. Comparison of off-axis crustal thickness variations between individual segments does not yield a strong correlation between the magmatic "pulses" in individual segments and time. If these crustal thickness variations reflect changes in melt production, this result suggests that there is not a strong interdependence in the amount of melt delivered to the axis, even in adjacent spreading segments. In addition, with the exception of segment 1S, the variations in crustal thickness are not symmetrical with respect to the axis. Thus if pulses in melt production are responsible for the across-axis variations in the residual gravity field, the asymmetry about the axis in crustal thickness undulations is indicative of asymmetry in lithospheric extension or mantle upwelling. Structural studies along the Mid-Atlantic Ridge have indicated that the rift valley is in general asymmetric in cross section and that half-grabens may be the fundamental building blocks of segments (e.g., *Mutter and Karson [1992]*). However, asymmetric lithosphere extension occurs predominantly at the end of segments and not at their midpoints and this is unlikely to explain our observation. Asymmetric upwelling may result from the presence of offsets along the plate boundary [*Rabinowicz et al., 1993*] and may explain the asymmetric distribution of crustal thickness undulations about the spreading center.

In addition to crustal thickness variations, a potential source for the across-axis variations in the gravity anomaly could be changes in crustal densities. If we use a model of constant crustal thickness, the average density of the crust would have to decrease substantially (from 2730 kg m⁻³ the value used in our Bouguer corrections, to 2530 kg m⁻³) to account for the observed residual gravity anomaly lows. Previous observations show that hydrothermal alteration can reduce the density of crustal rocks (e.g., *Gillis et al. [1993]*) with low temperature alteration having a more significant effect than high-temperature alteration. However, physical property studies of dikes and gabbros from drillholes in the Troodos ophiolite and from ODP holes 504B (~ 6 Ma crust) and 735B (~ 12 Ma crust) indicate that the average density of these crustal rocks, including zones of alteration, is > 2900 kg m⁻³ [*Smith and Vine, 1989; Iturrino et al., 1991; Dick et al., 1992*]. Since the dikes and gabbros are likely to comprise the bulk of the crust (especially at the midpoint of a spreading segment), we expect them to dominate the density structure of oceanic crust. We think it is unlikely that hydrothermal alteration can reduce the average crustal density by the amount required to account for the gravity anomalies which have a wavelength of ~ 35 km along the midpoint traces.

Conclusions

Our analysis of gravity data over the axis of the Mid-Atlantic Ridge between 29°N and 31° 30'N shows that, after accounting for the density contrast at the seafloor and for lithospheric cooling, there are substantial variations in the residual gravity anomaly both along- and across-axis. Our main conclusions are as follows:

1. The variations in crustal thickness that we have computed based on the residual gravity anomaly to first order reflect the present and past pattern of segmentation of the plate boundary within our survey area. For the two segments south of the Atlantis Fracture Zone, computed crustal thickness values are high near segment midpoints and low near segment discontinuities. This relationship is maintained out to 10 Ma suggesting that segment discontinuities reflect long-term boundaries between centers of focused mantle upwelling. For the segments north of the Atlantis Fracture Zone, the consistent association of thin crust with segment end points, and thick crust with segment midpoints is observed only in crust less than ~3 Ma. This result suggests that (1) focused mantle upwelling has only recently been initiated north of the Atlantic Fracture Zone, or (2) occurred at a scale smaller than we can resolve (~ 25 km). The onset of focused mantle upwelling in lithosphere younger than 3 Ma is coincident with change in the geometry of the plate boundary and appears to be related to a change in spreading direction [*Sempéré et al., 1995*].

2. Computed crustal thickness gradually decreases with age in a few segments in our study area. We propose that this "apparent" crustal thinning is a result of lateral changes in mantle density not predicted by the passive flow model used in our study. These lateral changes in mantle density are most likely related to buoyant upwelling and focusing of flow, and can result in a decrease in the residual gravity field close to the spreading center.

3. Variations in computed crustal thickness on a timescale of 2-3 m.y. may be due to temporal variations in melt production and suggest that some nonsteady state behavior, for example pulses in magma production, has occurred. Comparison of off-axis crustal thickness variations between individual segments does not yield a strong correlation between the "pulses" in individual segments and time. Thus if the crustal thickness variations do reflect magma pulses, there is little interdependence in the amount of melt delivered to the axis even in adjacent spreading segments.

Acknowledgments. We are very grateful to P. Patriat, L. Géli, L. Parson, B. West for many fruitful discussions. We would like to thank Captain J. O'Loughlin and the crew of the R/V *Maurice Ewing* of Columbia University for their assistance during the field program. We are also indebted to D. Chayes, D. Caress, and S. O'Hara who provided software to acquire and process the Hydrosweep bathymetric data, and to S. Budhypramono and J. Stennett for their invaluable help at sea. The GMT software package was used extensively throughout this study (*Wessel and Smith, 1991*). This study was funded by the National Science Foundation (contract OCE-9017975). C. Rommevaux was funded by Géosciences Marines INSU (933911).

References

- Blackman, D. K., and D.W. Forsyth, Isostatic compensation of tectonic features of the Mid-Atlantic Ridge 25°-27°30' S, *J. Geophys. Res.*, 96, 11,741-11,758, 1991.
- Chayes, D.N., Hydrosweep-DS on the R/V *Ewing*, *IEEE Oceanic Eng.*, 737-742, 1992.

- Cormier, M.-H., R. S. Detrick, and G. M. Purdy, Anomalous thin crust in oceanic fracture zones: New seismic constraints from the Kane fracture zone, *J. Geophys. Res.*, **89**, 10,249-10,266, 1984.
- Detrick, R.S., H.D. Needham, and V. Renard, Gravity anomalies and crustal thickness variations along the Mid-Atlantic Ridge between 33°N and 40°N, *J. Geophys. Res.*, **100**, 3767-3787, 1995.
- Dick, H.J.B., et al., *Proc. Ocean Drill. Program Initial Rep.*, **140**; 106-108, 1992.
- Gente, P., et al., Geometry of past and present-day segmentation of the Mid-Atlantic Ridge south of Kane fracture zone, *Eos Trans. AGU*, **72** (44), 476-477, Fall Meet-suppl., 1991.
- Gillis, K., et al., *Proc. Ocean Drill. Program Initial Rep.*, **147**, 98-100, 1993.
- Iturrino, G.J., N.I. Christensen, S. Kirby, and M.H. Salisbury, Seismic velocities and elastic properties of gabbroic rocks from Hole 735B, *Proc. Ocean Drill. Program, Sci. Results*, **118**, 227-237, 1991.
- Karson, J.A., and A.T. Winters, Along-axis variations in tectonic extension and accommodation zones in the MARK area, Mid-Atlantic Ridge 23° N Latitude, In *Ophiolites and Their Modern Oceanic Analogues*, edited L.M. Parson, B.J. Murton, and P. Browning, *Geol. Soc. Spec. Publ. London*, Blackwell Scientific Publications, 107-116, 1992.
- Kuo, B.-Y., and D.W. Forsyth, Gravity anomalies of the ridge-transform system in the South Atlantic between 31 and 34.5° S: Upwelling centers and variations in crustal thickness, *Mar. Geophys. Res.*, **10**, 205-232, 1988.
- Lin, J., and E.A. Bergman, Rift grabens, seismicity and volcanic segmentation of the Mid-Atlantic Ridge: Kane to Atlantis Fracture Zone, *Eos Trans. AGU*, **71** (43), 1572, 1990.
- Lin, J., and J. Phipps Morgan, The spreading rate dependence of 3-D mid-ocean ridge structure, *Geophys. Res. Lett.*, **19**, 13-16, 1992.
- Lin, J., G.M. Purdy, H. Schouten, J.-C. Sempéré, and C. Zervas, Evidence from gravity data for focused magmatic accretion along the Mid-Atlantic Ridge, *Nature*, **344**, 627-632, 1990.
- Macdonald, K.C., P.J. Fox, L.J. Perram, M.F. Eisen, R.M. Haymon, S.P. Miller, S.M. Carbotte, M.-H. Cormier, and A.N. Shor, A new view of the mid-ocean ridge from the behaviour of the ridge axis-discontinuities, *Nature*, **335**, 217-255, 1988.
- Morris, E., and R.S. Detrick, Three-dimensional analysis of gravity anomalies in the MARK area, Mid-Atlantic Ridge 23° N, *J. Geophys. Res.*, **96**, 4355-4366, 1991.
- Mutter, J. C., and J. Karson, Structural processes at slow-spreading ridges, *Science*, **257**, 627-634, 1992.
- Needham, H. D., et al., The crest of the Mid-Atlantic Ridge between 40°N and 15°N: Very broad swath mapping with the EM12 echosounding system, *Eos Trans. AGU*, **72** (44), 470, Fall Meet. suppl., 1991.
- Neumann, G.A., and D.W. Forsyth, The paradox of the axial profile: Isostatic compensation along the axis of the Mid-Atlantic Ridge?, *J. Geophys. Res.*, **98**, 17,891-17,910, 1993.
- Parsons, B., and J.G. Sclater, An analysis of the variation of ocean floor bathymetry and heat flow with age, *J. Geophys. Res.*, **82**, 803-827, 1977.
- Phillips, J. D., and H. S. Fleming, Multibeam sonar study of the Mid-Atlantic Ridge rift valley 36-37°N, *Geol. Soc. Am. Bull.*, **88**, 1-5, 1977.
- Phipps Morgan, J., and D.W. Forsyth, Three-dimensional flow and temperature perturbations due to a transform offset: Effects on oceanic crustal and upper mantle structure, *J. Geophys. Res.*, **93**, 2955-2966, 1988.
- Prince, R. A., and D.W. Forsyth, Horizontal extent of anomalously thin crust near the Vema Fracture Zone from the three-dimensional analysis of gravity anomalies, *J. Geophys. Res.*, **93**, 8051-8063, 1988.
- Purdy, G. M., J.-C. Sempéré, H. Schouten, D. Dubois, and R. Goldsmith, Bathymetry of the Mid-Atlantic Ridge, 24°-31° N: A map series, *Mar. Geophys. Res.*, **12**, 247-252, 1990.
- Rabinowicz, M., S. Rouzo, J.-C. Sempéré and C. Rosemberg, Three-dimensional models of mantle flow beneath spreading centers, *J. Geophys. Res.*, **98**, 7851-7869, 1993.
- Ramberg, I.B., D.F. Gray, and R.G.H. Reynolds, Tectonic evolution of the FAMOUS area of the Mid-Atlantic Ridge, lat. 35°50'N to 37°20'N, *Geol. Soc. Am. Bull.* **88**, 609-620, 1977.
- Rommevaux, C., C. Deplus, P. Patriat, and J.-C. Sempéré, Three-dimensional gravity study of the Mid-Atlantic Ridge: Evolution of the segmentation between 28°N and 29°N during the last 10 Ma, *J. Geophys. Res.*, **99**, 3015-3029, 1994.
- Rona, P.A., and D.F. Gray, Structural behavior of fracture zones symmetric and asymmetric about a spreading axis: Mid-Atlantic Ridge, *Nature*, **321**, 33-37, 1980.
- Rona, P.A., R. N. Harbison, B. G. Bussinger, R. B. Scott, and A. J. Natwalk, Tectonic fabric and hydrothermal activity of the Mid-Atlantic Ridge crest (lat 26°N), *Geol. Soc. Am. Bull.*, **87**, 661-674, 1976.
- Schouten, H., H. J. B. Dick, and K. D. Klitgord, Migration of mid-ocean ridges, *Nature*, **326**, 835-839, 1987.
- Scott, D. R., Small-scale convection and mantle melting beneath mid-ocean ridges, in *Mantle Flow and Melt Generation at Mid-Ocean Ridges*, *Geophys. Monogr. Ser.*, Vol. 71, edited by J. Phipps Morgan, D. K. Blackman, and J. M. Sinton, pp. 327-352, AGU, Washington, D. C., 1992.
- Searle, R.C., and A.S. Loughton, Sonar studies of the Mid-Atlantic Ridge and Kurchatov Fracture Zone, *J. Geophys. Res.*, **82**, 5313-5328, 1977.
- Sempéré, J.-C., Tectonic variations along the axis of the Mid-Atlantic Ridge: Observations and finite-element modelling (abstract), *Eos Trans. AGU*, **72** (44), 471, Fall Meet. suppl., 1991.
- Sempéré, J.-C., G.M. Purdy, and H. Schouten, Segmentation of the Mid-Atlantic Ridge between 24°N and 30° 40'N, *Nature*, **344**, 427-431, 1990.
- Sempéré, J.-C., J. Lin, H.S. Brown, H. Schouten, and G.M. Purdy, Segmentation and morphotectonic variations along a slow-spreading center: The Mid-Atlantic Ridge (24° 00' N - 30° 40' N), *Mar. Geophys. Res.*, **15**, 153-200, 1993.
- Sempéré, J.-C., et al., The Mid-Atlantic Ridge between 29° N and 31° 30' N in the last 10 Ma, *Earth Planet. Sci. Lett.*, **130**, 45-55, 1995.
- Shaw, P.R., Ridge segmentation, faulting, and crustal thickness in the Atlantic, *Nature*, **358**, 490-493, 1992.
- Shen, Y.S., and D.W. Forsyth, The effects of temperature- and pressure-dependent viscosity of three-dimensional passive flow of the mantle beneath a ridge-transform system, *J. Geophys. Res.*, **97**, 19-717-19,728, 1992.
- Sloan, H., and P. Patriat, Kinematics of the North American-African plate boundary between 28° and 29° during the last 10 Ma: Evolution of the axial geometry and spreading rate and direction, *Earth and Planet. Sci. Lett.*, **113**, 323-341, 1992.
- Smith, G.C., and F.J. Vine, The physical properties of diabases, gabbros, and ultramafic rocks from C.C.S.P. drill hole CY-4 at Palekori, Cyprus, in *Cyprus Crustal Study Project: Initial Report, Hole CY-4*, edited by I.L. Gibson, J. Malpas, P.T. Robinson, and C. Xenophontos, *Pap. Geol. Surv. Can.*, **88-9**, 295-314, 1989.
- Smith, W. H. F., and P. Wessel, Gridding with continuous curvature splines in tension, *Geophysics*, **55**, 293-305, 1990.
- Su, W., and W. R. Buck, Buoyancy effects on mantle flow under mid-ocean ridges, *J. Geophys. Res.*, **98**, 12,191-12,205, 1993.
- Su, W., C. Z. Mutter, J. C. Mutter, and W. R. Buck, Some theoretical predictions on the relationships among spreading rate, mantle temperature, and crustal thickness, *J. Geophys. Res.*, **99**, 3215-3227, 1994.
- Tolstoy, M., A. J. Harding, and J. A. Orcutt, Crustal thickness on the Mid-Atlantic Ridge: Bull's eye gravity anomalies and focused accretion, *Science*, **262**, 726-729, 1993.
- Turcotte, D. L., and J. Phipps Morgan, The physics of magma migration and mantle flow beneath a mid-ocean ridge, in *Mantle Flow and Melt Generation at Mid-Ocean Ridges*, *Geophys. Monogr. Ser.*, Vol. 71, edited by J. Phipps Morgan, D. K. Blackman, J. M. Sinton, pp. 155-181, AGU, Washington, D. C., 1992.
- Wessel, P., and W. H. F. Smith, Free software helps map and display data, *Eos Trans. AGU*, **72** (44), 489, Fall Meet. Suppl., 1991.

J.E. Pariso and J.-C. Sempéré, School of Oceanography, University of Washington, Box 357940, Seattle, WA 98195-7940. (e-mail: Pariso@ocean.washington.edu and sempere@ocean.washington.edu)
 C. Rommevaux, Institut de Physique du Globe de Paris, CNRS, URA 729, 4 Place Jussieu, B.P. 89, 75252 Paris, Cedex 05, France. (e-mail: cer@ccr.jussieu.fr)

(Received June 22, 1994; revised March 31, 1995; accepted March 31, 1995.)